Convective System Dynamics Viewed in 3D over the Oceans

Tran Vu La[1] and Christophe Messager[1]

[1]EXWEXs

November 26, 2022

Abstract

A combination of Sentinel-1 and Meteosat datasets in recent studies of the same authors exhibited a link between sea surface wind patterns and deep convective clouds aloft. This observation strengthened the assumption that Convective System (CS) vertical downdrafts produce significant horizontal surface winds when they collide the sea surface. The Aeolus new observations may bring additional credits to this assumption by the measurements of vertical wind profiles. The combination of these three satellites (Sentinel-1, Aeolus, and Meteosat) with a slight lag in observation time illustrates the significant results of a (near) three-dimensional observation of the CS over the sea. They also indicate the matching in space and time apparition of deep convective clouds viewed by Meteosat, intense downdrafts viewed by Aeolus, and high surface winds estimated by Sentinel-1.

Convective System Dynamics Viewed in 3D over the Oceans

Tran Vu La[1], Christophe Messager[1]

[1]Extreme Weather Expertises (EXWEXs), 2 Rue de Kéraliou, 29200, Brest, France.

Corresponding author: Tran Vu La (tvl@exwexs.fr)

Key Points:

- Three-dimensional satellite observation of convective systems over the sea surface
- Combination of Sentinel-1, Aeolus, and Meteosat having the same orbits and acquisition time
- Matching of sea surface wind patterns, intense downdrafts, and deep convective clouds observed by Sentinel-1, Aeolus, and Meteosat

Abstract

A combination of Sentinel-1 and Meteosat datasets in recent studies of the same authors exhibited a link between sea surface wind patterns and deep convective clouds aloft. This observation strengthened the assumption that Convective System (CS) vertical downdrafts produce significant horizontal surface winds when they collide the sea surface. The Aeolus new observations may bring additional credits to this assumption by the measurements of vertical wind profiles. The combination of these three satellites (Sentinel-1, Aeolus, and Meteosat) with a slight lag in observation time illustrates the significant results of a (near) three-dimensional observation of the CS over the sea. They also indicate the matching in space and time apparition of deep convective clouds viewed by Meteosat, intense downdrafts viewed by Aeolus, and high surface winds estimated by Sentinel-1.

Plain Language Summary

Cumulonimbus clouds (anvils or convective systems) may be associated with some meteorological hazards, including intense precipitation (up to 50 mm/hr), surface wind gust (exceeding 25 m/s), and strong lightning. For a long time, the analyses and prediction of cumulonimbus clouds and their effects over the surface have been generally complicated due to the lack of observation data, particularly when cumulonimbus clouds occur suddenly in a short time. The understanding and forecast of cumulonimbus have been much improved in recent years thanks to the launch of geostationary satellites (Meteosat, GOES, Himawari) that cover the entire earth with a 5-10 minutes time sampling. Likewise, surface wind patterns associated with cumulonimbus clouds can be observed by the low altitude polar satellites and especially by Sentinel-1 SAR (Synthetic Aperture Radar) satellites at a high spatial resolution. Furthermore, the launch of the Aeolus satellite on August 22nd, 2018 enables the observations of the section of vertical wind profiles associated with surface wind gust viewed by Sentinel-1. The combination of three satellites (Sentinel-1, Aeolus, Meteosat) offers a 3D observation of cumulonimbus clouds aloft (15 km high) and the associated wind gust over the sea surface. The current study indicates that the production of surface wind gust depends on the intensity of the downward air flux from the higher cumulonimbus altitude to the sea surface.

1 Introduction

Convective Systems (CS) are dangerous mesoscale and sub-mesoscale meteorological events as they are associated with lightning, intense precipitation, and strong surface wind gust (Mohr et al., 2017; Kastman et al., 2017). In particular, it is hard to predict the CS due to their sudden presence and fast development. While the CS may occur everywhere, the most intensive ones regularly occur in the tropics (for instance, in the Gulf of Guinea or Southeast Asia), and the observation and forecast of the whole CS dynamics remain a significant challenge. However, thanks to some performing geostationary satellites (Meteosat, GOES, Himawari, Gaofen-1, which observe Europe and Africa, America, and Asia, respectively), the progress in real-time observations enables significant improvement in CS track. However, the sensors onboard these geostationary satellites do not let a direct observation of atmospheric dynamics (horizontal and vertical winds, for instance). Instead, part of the thermodynamics may be retrieved (brightness temperature, water content). As a result, the detection and observation of the vertical CS dynamics, as well as its direct effects on the sea surface via the CS downdrafts hitting the surface are still an issue. According to King et al. (2017) and Priftis et al. (2018), the C-band scatterometers (ASCAT-A/B) may estimate high surface wind speed associated with the CS. However, Kilpatrick and Xie (2015) highlighted that ASCAT may only detect surface wind patterns not exceeding 15 m/s produced by the 100–300 km mesoscale downdrafts. Additionally, they cannot reach the 5-20 km convective-scale gust fronts associated with wind magnitude of 20 to 25 m/s, due to their too coarse spatial resolution. As a result, La et al. (2018, 2020a, 2020b) proposed a new method based on the use of the high-resolution Synthetic Aperture Radar (SAR) images (C-band Sentinel-1 and Radarsat-2) for the detection of surface wind patterns associated with CS.

Thanks to the Sentinel-1 high spatial resolution and large swath, various types of wind patterns were observed in La et al. (2018, 2020a, 2020b), including mesoscale and sub-mesoscale squall lines, and mesoscale convection cells. The wind intensity of these patterns varied from 10–25 m/s. The spots with high winds (15–25 m/s) were observed on the high-resolution Sentinel-1 images while not reported with ASCAT. Moreover, these studies highlighted the location matching (even agreement in shape) between deep convective clouds (with 200°-210°K brightness temperature) observed by Meteosat and surface wind patterns on Sentinel-1 images. This observation strengthened the assumption that wind patterns with 10-25 m/s were produced by the downdrafts associated with deep convective clouds hitting the sea surface. However, before the Aeolus data (Stoffelen et al., 2020), there were no reliable ways to observe and relate vertical and horizontal winds to verify this assumption.

Being launched on August 22nd, 2018, Aeolus is the first satellite with sensors able of performing vertical wind-component-profile observations. To estimate vertical wind intensity, the receivers integrated on the Aeolus satellite measure the frequency shift of the laser light emitted from the Lidar then backscattered by aerosol and molecules. The combination of the two channels (based on aerosol and molecular laser signal interferences) enables vertical wind intensity estimation from 27 km high to the surface with layers of 0.5, 1.0, and 2.0 km thickness.

Compared to the previous studies led by La et al. (2018, 2020a, 2020b), the current paper proposes the addition of Aeolus data to characterize the 3D dynamics of the CS over the sea. This study will focus on the Gulf of Guinea region (shown in Figure 2), where the CS occur regularly from November to June (Sultan et al., 2003; Raj et al., 2018).

Section 2 presents the methodology, including the selection of Sentinel-1, Aeolus, and Meteosat images (having matching orbits) and data processing. Section 3 illustrates a 3D CS observation on May 31st, 2020. Section 4 talks about conclusions and perspectives.

2 Methodology

2.1 Combination of Sentinel-1, Aeolus, and Meteosat

The actual work is based on the combination of Meteosat, Aeolus, and Sentinel-1 for the detection of deep convective clouds, the associated downdrafts, and resulting sea surface wind patterns, respectively, as shown in Figure 1. As a result, a (nearly) 3D view of an active CS may be delivered with a marine surface view of winds, the associated vertical section of winds, and deep convection aloft.

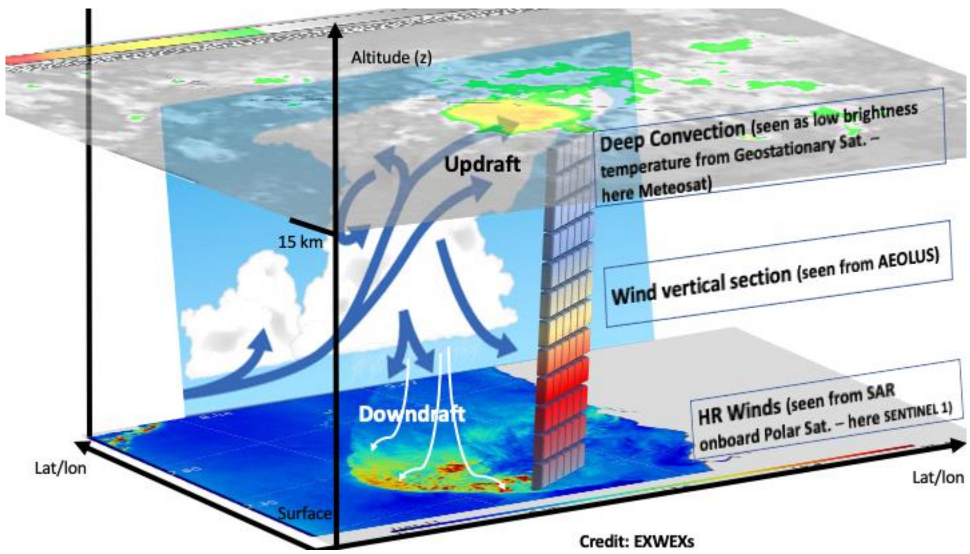

Figure 1. 3D view of a convective system with the coldest deep convection at 15 km high (viewed by Meteosat), intense downdrafts at midlevels and near the sea surface (viewed by Aeolus), and surface wind patterns associated with the intense downdrafts (observed by Sentinel-1).

The revisit time of Sentinel-1 (3-5 days) and Aeolus (two cycles per day) in the Gulf of Guinea enables the selection of images having time and space matching footprints.

Figure 2 presents the Sentinel-1 images with vertical dual-polarization acquired from May 1st to 31st, 2020 over the Gulf of Guinea. The images are High Resolution (HR) Interferometric Wide Swath (IWS) products with 10 m pixel spacing and 250 km swath, which enables the observation of sea surface wind patterns at multiple scales following the approach of La et al. (2018, 2020a, 2020b). Figure 2 also illustrates the footprints of Aeolus over this region on May 31st, 2020, including ascending and descending orbit directions. These footprints are mainly observed around 05:00 UTC for the descending direction and around 18:00 UTC for the ascending one. This time also corresponds to that of Sentinel-1 over the same footprints. As a result, the observation time lag between Sentinel-1 and Aeolus is lower than 15 minutes. Likewise, the whole time lag of image acquisitions between Sentinel-1, Aeolus, and Meteosat does not exceed 15 minutes since the sampling time of Meteosat is 15 minutes. For instance, Table 1 illustrates the acquisition time for Sentinel-1, Aeolus, and Meteosat, May 31st, 2020, over the Gulf of Guinea. The time lag between three satellites for this event does not exceed 10 minutes.

The event of May 31st, 2020 was selected among many others since Sentinel-1 and Aeolus have matching footprints over the region of interest (ascending orbit) and the time lag between them is short. Furthermore, the convection process in this case is characteristic of the CS in this region for this period. A mesoscale CS produces intense downdrafts hitting the ocean and then causing surface strong winds.

In addition to the typical deep convection illustrated here, some other cases were noticed in the study of 3D view of CS dynamics (not shown in the current paper). The intense downdrafts are observed in the mid-levels but disappeared near the sea surface, and thereby no surface wind gust is detected. Likewise, the organized mesoscale CS can cause high surface winds without downdrafts. Moderate (or weak) convective downdrafts present in the mid-levels can produce severe winds due to the impact of the parameters near the surface, or there is no surface wind pattern, despite intense downdrafts.

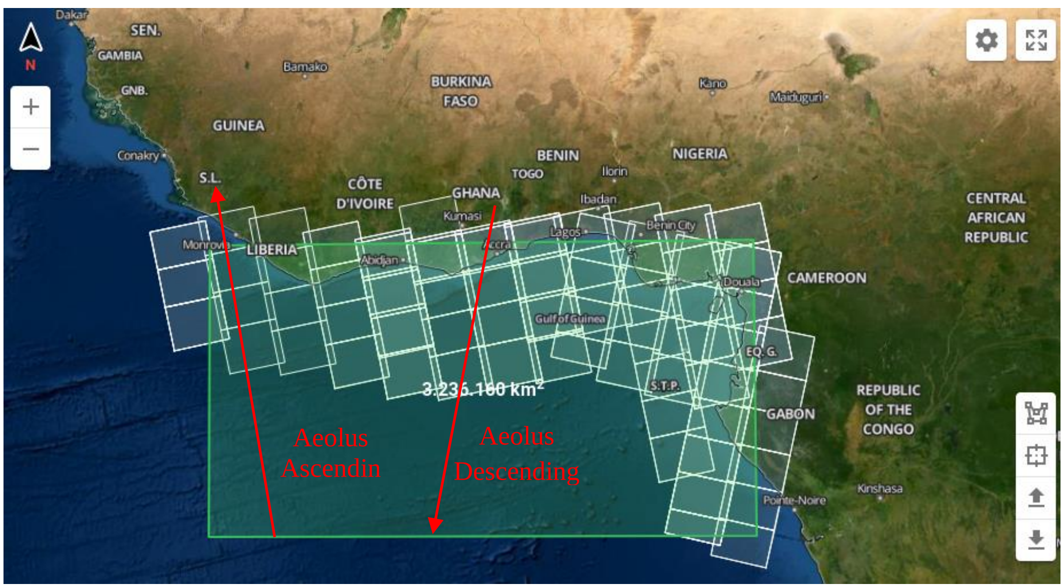

Figure 2. Region of interest (Gulf of Guinea) and Sentinel-1 images acquired from May 1st to 31st, 2020 in this region. It also illustrates the Aeolus ascending and descending orbits (red arrows), May 31st, 2020. (Credits: EXWEXs).

Table 1. Acquisition time (UTC) for Sentinel-1, Aeolus, and Meteosat, May 31st, 2020, over the Gulf of Guinea.

Date	Sentinel-1	Aeolus	Meteosat
May 31st, 2020	18:41:30-18:42:24	18:31-18:35	18:30-18 :45

2.2 Data processing

La et al. (2018, 2020a, 2020b) illustrated that surface wind patterns associated with the CS may be detected on Sentinel-1 SAR images. The normalized radar cross section (NRCS) and incident angle obtained from Sentinel-1 images and the extracted wind direction from the Global Forecast System (GFS) data were used in CMOD5.N (Hersbach, 2008) for surface wind speed estimation. The CMOD5.N function was selected since it may compute wind intensity estimates up to 25 m/s (Mouch et al., 2017), which is usual for the CS-associated wind patterns.

Vertical wind intensity presented in this paper is given by the Rayleigh receiver of Aeolus based on the measurements of air-particle backscattering from 27 km high to the surface with unevenly-divided thickness layers of 2 km, 1 km, and finally 0.5 km for the stratosphere, troposphere, and planetary boundary layer, respectively.

Meteosat images with a 2.8 km spatial resolution are used for the detection of deep convective clouds based on low brightness temperature (200°K-230°K). The deeper the convective clouds, the lower the brightness temperature is. La et al. (2018, 2020a, 2020b) indicated that the coldest convective spots corresponded to the highest wind intensity of ocean surface wind patterns. Meteosat images are also used for the extraction of cloud top height to compare with that of Aeolus vertical wind profile observations. The ones having the same observation time as Sentinel-1 are resampled on the grids of the latter to facilitate the comparisons between them.

3 Convective system observation under three dimensions

Figure 3 illustrates the 3D observation of a CS, May 31st, 2020, based on the surface wind pattern on the Sentinel-1 image (Figure 3a), the vertical wind intensity from the Aeolus measurements (Figure 3b), the deep convective cloud (Figures 3c-3d), and the cloud top height on the Meteosat image (Figure 3e). The acquisition time of these images was reported in Table 1.

Figure 3a presents a mesoscale surface wind pattern (6.6°W-4.8°W, 1°N-2.4°N) with wind intensity 10-25 m/s, and Figures 3c-3d illustrates a deep convective cloud with the brightness temperature less than 220°K at the same locations (18:30 and 18:45 UTC, respectively). This spatial matching is particularly well noticed for the coldest convective spots at 200-205°K in Figure 3c with the significant surface wind intensity patterns (20-25 m/s) in Figure 3a. They have not only the same location (6.6°W-6°W, 1.8°N-2.1°N) but also a similar size. As indicated by La et al. (2018, 2020a, 2020b), the relationship between the mesoscale surface wind patterns in Figure 3a and the deep convective clouds in Figure 3c suggests a direct dynamics link between deep convection producing intense downdrafts and then inducing surface wind fronts and wind patterns.

Between Figures 3c and 3d (with 15 minutes lag), the convective clouds move very slowly. They almost do not change their shape and position. This is (probably) because the synoptic winds at 850-300 hPa (Corfidi et al., 1996), one of the factors affecting significantly the CS movement speed, have low intensities. However, the coldest spot at 200-205°K evolves its shape, but (very) little about the position. This exhibits that the thermodynamics process of this convection still occurs actively; however, it may not be strong enough to decide the CS movement speed while the synoptic winds are weak.

In Figure 3b, Sentinel-1 and Aeolus highlight some matching footprints with a short time lag (about 10 minutes). Indeed, four Aeolus (horizontal) data parcels (about 400 km) correspond to the footprint length of the Sentinel-1 image (0°N-3.7°N). Near the sea surface, several intense vertical downward winds (-40 m/s) are observed at the same spatial locations as the wind pattern on the sea surface in Figure 3a and as the deep convective cloud aloft in Figure 3c. This suggests that the surface winds in Figure 3a are (likely) produced by these intense downward winds themselves associated with the deep cold cloud in Figure 3c.

Also, Figure 3e presents the convective cloud top heights (12.5-15 km) shown in Figure 3c. The coldest clouds with 200-205°K (2°N, 6.7°W-5.9°W) exhibit close altitudes (about 15 km high) to the ones measured by Aeolus (Figure 3b). This kind of deep convection is very usual over West Africa where the derived solar tropical energy is quite enough to trigger and enhance strong deep convection that may reach easily 12-16 km altitude with even overshooting of the tropopause at 20 km high (Houze, 2004; Xu and Randall, 2001; Cotton et al., 2011). For instance, based on the CloudSat-CALIPSO satellite over West Africa, Bourgeois et al. (2018) illustrated the deep convective clouds up to 15 km high. Also, using the same dataset, Hagihara et al. (2014) observed the identical deep convective clouds at the same altitude but over the North Atlantic Ocean.

The combination of Sentinel-1, Aeolus, and Meteosat in Figure 3 illustrates a kind of 3D CS observation over the sea close to the schematic understanding of CS dynamics and the associated strong surface winds. The corresponding Meteosat and Aeolus images (Figures 2b, 2c, and 2d) indicate that several intense vertical winds representative of the CS-associated downdrafts are formed at the high altitude (about 15 km high) and then accelerate in the midlevels and near the surface, according to the thermo-dynamical conditions. When these downdrafts hit the sea surface, they spread mostly anisotropically (towards the CS movement direction) and produce surface winds from moderate to high intensity, as shown in Figure 3a, depending on the downdraft intensity and the near-surface atmospheric conditions.

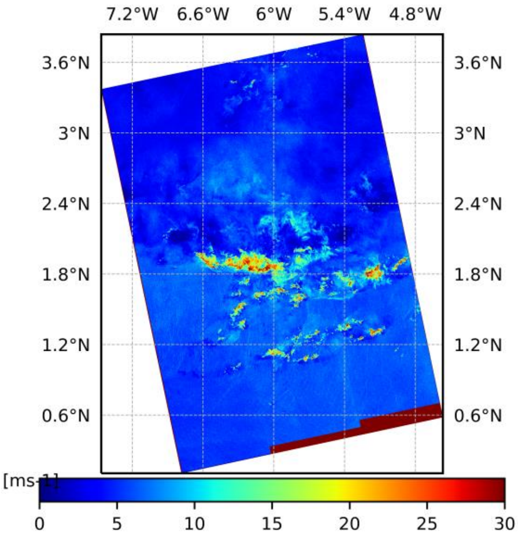
7.2°W
6.6°W
6°W
5.4°W
4.8°W
3.6°N
3°N
2.4°N
1.8°N
1.2°N
0.6°N
[ms-1]
0
5
10
15
20
25
30

(a)

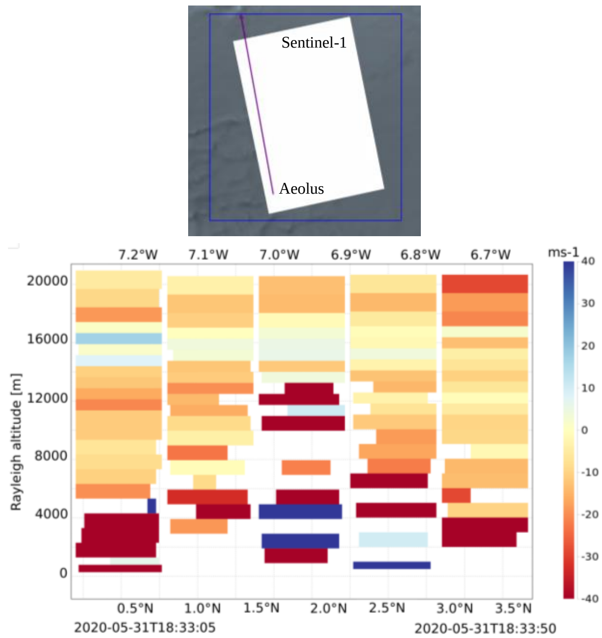
Sentinel-1
Aeolus
7.2°W
7.1°W
7.0°W
6.9°W
6.8°W
6.7°W
ms-1
Rayleigh altitude [m]
20000
16000
12000
8000
4000
0
0.5°N
1.0°N
1.5°N
2.0°N
2.5°N
3.0°N
3.5°N
2020-05-31T18:33:05
2020-05-31T18:33:50
40
30
20
10
0
-10
-20
-30
-40

(b)

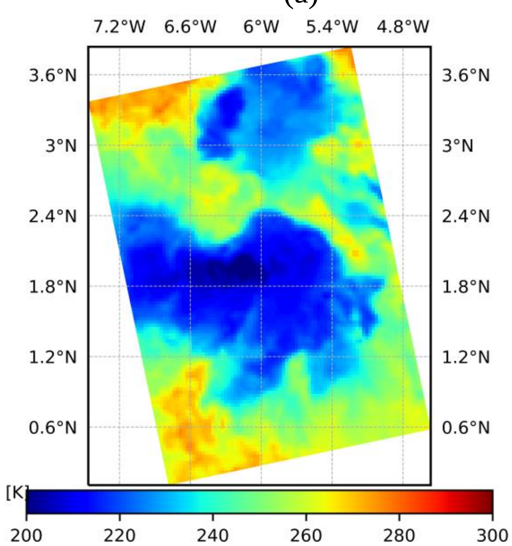
7.2°W
6.6°W
6°W
5.4°W
4.8°W
3.6°N
3°N
2.4°N
1.8°N
1.2°N
0.6°N
[K]
200
220
240
260
280
300

(c)

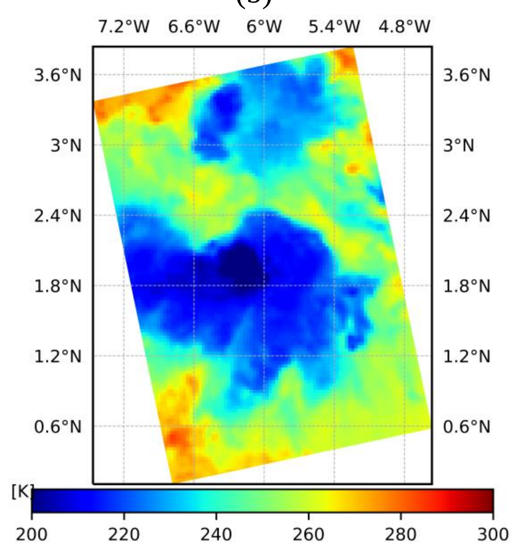
7.2°W
6.6°W
6°W
5.4°W
4.8°W
3.6°N
3°N
2.4°N
1.8°N
1.2°N
0.6°N
[K]
200
220
240
260
280
300

(d)

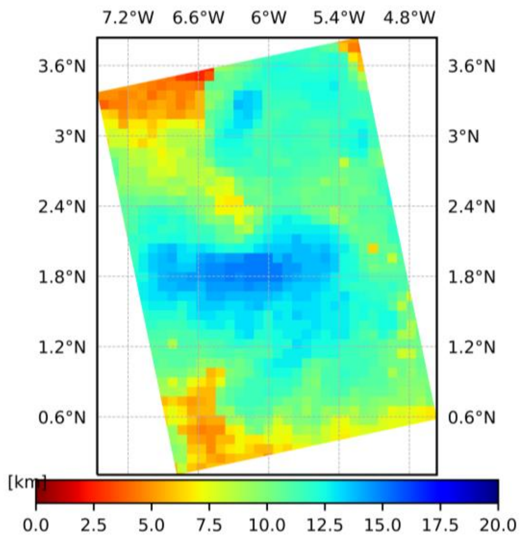

(e)

Figure 3. Multi-view observation of a CS, May 31st, 2020, based on (a) surface wind pattern (10-25 m/s wind speed) on Sentinel-1 image (18:41:30-18:42:24 UTC), (b) vertical section of wind intensity (m/s) from Aeolus measurements (18:33:05 - 18:33:50 UTC) corresponding to Sentinel-1 image (the missing data are due to the dense water clouds), (c, d) brightness temperature fields highlighting deep convection at 200°K-230°K (18:30 and 18:45 UTC, respectively), and (e) cloud top height on Meteosat image (18:30 UTC).

4 Conclusions

The current paper illustrates, for the first time, a (near) 3D observation of CS dynamics (horizontal and vertical winds) over the sea, based on the combination of three satellites (Sentinel-1, Aeolus, Meteosat) with a short time lag (about 10 minutes). In the studied case of May 31st, 2020, surface wind patterns with moderate and high winds (10–25 m/s) detected by Sentinel-1 correspond to deep convective clouds (200–230°K brightness temperature) observed by Meteosat, and especially to intense vertical winds from 12.5-15 km high to near the sea surface. This observation follows the schematic CS dynamics: a downdraft that occurs from precipitation loading and evaporative cooling in a convective cloud will become intense through the midlevel and near the surface if the thermo-dynamical conditions are favorable. When the intense downdraft hits the sea surface, it may produce wind gust up to 25 m/s as indicated in the papers cited above.

More generally, the relationship between deep convective clouds, the associated vertical dynamics, and ocean surface wind gust remains a particular issue. The combination of these three satellites is thus a new and additional way of the CS dynamics observation that may be used not only for the monitoring of CS severity in real-time but also for data inclusion in the mesoscale assimilation models to improve the mesoscale CS initialization within forecast systems.

In a research topic, the method described here should lead to document many CS types and their variability in terms of deep convection, vertical dynamics as well as their effects at the sea surface. Finally, combining the three sources of data should lead to a better understanding of the CS dynamics itself.

Also, the CloudSat-CALIPSO data may be combined with the images of Sentinel-1, Aeolus, and Meteosat to bring new information about dynamics and dispersions offered by the aerosol observations.

Acknowledgments

This work is supported by the CNES (Centre National d'Etudes Spatiales) in the framework of the PEPS (La Plateforme d'Exploitation des Produits Sentinel) program. Sentinel-1A/B images are given by the European Copernicus Program. Meteosat images are provided by the European Organization for the Exploitation of Meteorological Satellites (EUMETSAT). The Aeolus data are downloaded via the virtual research platform VirES (https://aeolus.services/).

References

Mohr, S., Kunz, M., Richter, A., & Ruck, B. (2017), Statistical characteristics of convective wind gusts in Germany. *Nat. Hazards Earth Syst. Sci.*, *17*, 957–969. doi:10.5194/nhess-17-957-2017.

Kastman, S. J., Market, S. P., Fox, I. N., Foscato, A. L., & Lupo, R. A. (2017), Lightning and Rainfall Characteristics in Elevated vs. Surface Based Convection in the Midwest that Produce Heavy Rainfall. *Atmosphere 2017*, *8*(2), 36. doi:10.3390/atmos8020036.

King, G. P., Portabella, M., Lin, W., & Stoffelen, A. (2017), Correlating extremes in wind and stress divergence with extremes in rain over the Tropical Atlantic. *EUMETSAT Ocean and Sea Ice SAF Scientific Report* (OSI_AVS_15_02).

Priftis, G., Lang, T. J., & Chronis, T. (2018), Combining ASCAT and NEXRAD retrieval analysis to explore wind features of mesoscale oceanic systems. *Journal of Geo. Res.: Atmospheres*, *123* (10), 341–10, 360. doi.org/10.1029/2017JD028137.

Kilpatrick, T. J., & Xie, S-P. (2015), ASCAT observations of downdrafts from mesoscale convective systems. *Geophys. Res. Lett.*, *42*, 1951–1958. doi:10.1002/2015GL063025.

La, T. V., Messager, C., Honnorat, M., & Channelliere, C. (2018), Detection of convective systems through surface wind gust estimation based on Sentinel-1 images: A new approach. *Atmos Sci Lett.*, 19:e863. doi:10.1002/asl.863.

La, T. V., & Messager C. (2020), Convective system sea surface wind pattern detection and variability observation from a combination of Sentinel-1 and Radarsat-2 images. *Rem. Sens. Letters*,*11*(5), 446–454. doi:10.1080/2150704X.2020.1731621.

La, T. V., Messager, C., Honnorat, M., Sahl, R., Khenchaf, A., Channelliere, C., & Lattes, P. (2020), Use of Sentinel-1 C-Band SAR Images for Convective System Surface Wind Pattern Detection. *J. Appl. Meteor. Climatol.* doi:10.1175/JAMC-D-20-0008.1.

Stoffelen, A., and Coauthors, Wind profile satellite observation requirements and capabilities. *Bull. Amer. Meteor. Soc.*, doi: https://doi.org/10.1175/BAMS-D-18-0202.1.

Sultan, B., & Janicot, S. (2003), The West African Monsoon Dynamics. Part II: The “Preonset” and “Onset” of the Summer Monsoon. *J. Climate*, *16*, 3407–3427, doi:10.1175/1520-0442(2003)016<3407:TWAMDP>2.0.CO;2.

Raj, J., Bangalath, H. K., & Stenchikov, G. (2019), West African Monsoon: current state and future projections in a high-resolution AGCM. *Climate Dynamics*, *52*, 6441–6461. doi:10.1007/s00382-018-4522-7.

Hersbach, H. (2008), CMOD5.N: A C-band geophysical model function for equivalent neutral wind. *ECMWF Reading*, UK, Tech., Memo. 554.

Mouche, A. A., Chapron, B., Zhang, B., & Husson, R. (2017), Combined Co- and Cross-Polarized SAR Measurements Under Extreme Wind Conditions. *IEEE Trans. on Geo. & Rem. Sens.*, *55*(12), 6746–6755. doi: 10.1109/TGRS.2017.2732508.

Corfidi, S. F., Meritt, J. H., & Fritsch, J. M. (1996), Predicting the Movement of Mesoscale Convective Complexes. *Wea. Forecasting*, **11**, 41–46, https://doi.org/10.1175/1520-0434(1996)011<0041:PTMOMC>2.0.CO;2.

Houze, R. A. (2004), Mesoscale convective systems, *Rev. Geophys.*, *42*, RG4003, doi:10.1029/2004RG000150.

Xu, K., & Randall, D. A. (2001), Updraft and Downdraft Statistics of Simulated Tropical and Midlatitude Cumulus Convection. *J. Atmos. Sci.*, *58*, 1630–1649. doi: 10.1175/1520-0469(2001)058<1630:UADSOS>2.0.CO;2.

Cotton, W. R., Bryan, G., & van den Heever, S. C. (2011), Storm and Cloud Dynamics – The Dynamics of Clouds and Precipitating Mesoscale Systems, Chapter 9 – Mesoscale Convective Systems, *International Geophysics*, Academic Press, *99*, 455-526.

Bourgeois, E., Bouniol, D., Couvreux, F., Guichard, F., Marsham, J. H., Garcia-Carreras, L., Birch, C. E., & Parker, D. J. (2018), Characteristics of mid-level clouds over West Africa. *Q. J. R. Meteorol. Soc.*, *144*, 426-442. doi:10.1002/qj.3215.

Hagihara, Y., Okamoto, H., & Luo, Z. J. (2014), Joint analysis of cloud top heights from CloudSat and CALIPSO: New insights into cloud top microphysics, *J. Geophys. Res. Atmos.*, *119*, 4087–4106. doi:10.1002/2013JD020919.